

CoReS: Compatible Representations via Stationarity

Niccolò Biondi, Federico Pernici, Matteo Bruni, and Alberto Del Bimbo, *Senior Member, IEEE*

Abstract—In this paper, we propose a novel method to learn internal feature representation models that are *compatible* with previously learned ones. Compatible features enable for direct comparison of old and new learned features, allowing them to be used interchangeably over time. This eliminates the need for visual search systems to extract new features for all previously seen images in the gallery-set when sequentially upgrading the representation model. Extracting new features is typically quite expensive or infeasible in the case of very large gallery-sets and/or real time systems (i.e., face-recognition systems, social networks, life-long learning systems, robotics and surveillance systems). Our approach, called Compatible Representations via Stationarity (CoReS), achieves compatibility by encouraging stationarity to the learned representation model without relying on previously learned models. Stationarity allows features’ statistical properties not to change under time shift so that the current learned features are inter-operable with the old ones. We evaluate single and sequential multi-model upgrading in growing large-scale training datasets and we show that our method improves the state-of-the-art in achieving compatible features by a large margin. In particular, upgrading ten times with training data taken from CASIA-WebFace and evaluating in Labeled Face in the Wild (LFW), we obtain a 49% increase in measuring the average number of times compatibility is achieved, which is a 544% relative improvement over previous state-of-the-art.

Index Terms—Deep Convolutional Neural Network, Representation Learning, Compatible Learning, Fixed Classifiers.

1 INTRODUCTION

NATURAL intelligent systems learn in an open universe and can search and recognize concepts while improving their knowledge. Modern *artificial* intelligent systems typically perform visual search tasks exploiting internal feature representations learned by Deep Convolutional Neural Network (DCNN) models [1], [2], [3], [4]. The output of these models in response to an input image is commonly referred to as feature vector. Visual search is achieved by indexing large corpus of images (i.e., the *gallery-set*) according to their feature vectors and identifying the closest to a set of input images, called the *query-set*. The representation model is typically learned by exploiting another set of images, called the *training-set*. Successful examples of learning feature representation are: face-recognition [5], [6], [7], [8], [9], person re-identification [10], [11], [12], [13] and image retrieval [14], [15], [16], [17]. In the case in which these visual search systems receive novel data and/or want to adopt recent and more powerful network architectures, representation models may require to be *upgraded* to improve their recognition capabilities. However, DCNNs, when upgraded with novel data or with different architectures, must re-process all the images in the gallery-set to generate new features and replace the old ones to benefit from the upgrade. This process is known as *re-indexing*.

Many practical vision applications involve very large-gallery sets such as facial recognition systems and social networks. In a similar vein, artificial life-long learning systems and autonomous robotics systems may gather experiences throughout their lifetime using an external memory and

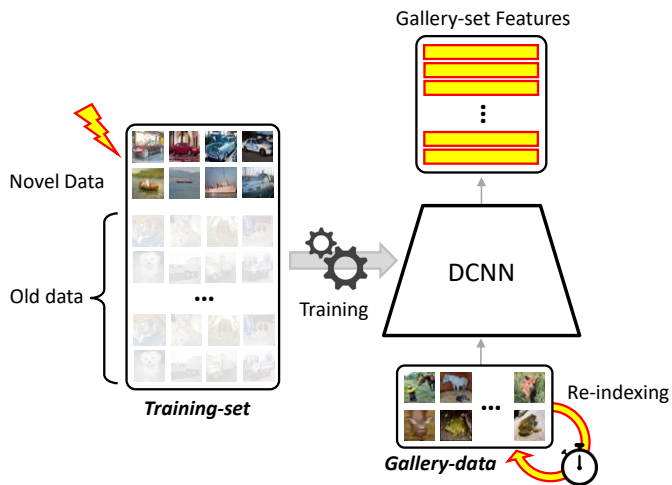


Fig. 1. Without compatible representation, updating the DCNN representation model with novel data requires all the gallery-set features to be re-indexed (the newly learned representation cannot be directly compared with the old one). Learning compatible representations allow direct feature comparison, thus eliminating the computationally intensive re-indexing of the gallery-set.

sequentially update¹ their internal representation [18], [19], [20]. The indexing process can therefore be computationally expensive or even infeasible (Fig. 1). Further problems may arise due to privacy or ethical concerns as the original gallery images could not be stored, thus making reprocessing impossible [21]. In this case, the previously computed feature vectors are the only viable solution to continue using

1. For new data assimilation, we use the term *upgrade* to denote learning a model from scratch and the term *update* to denote learning a model by fine-tuning a previous one.

the data.

In this paper, we propose a novel approach that avoids re-indexing the gallery-set during sequential upgrades of the representation model. The representation obtained in this manner is said to be *compatible* as the features before and after the learning upgrades can be directly compared. Learning compatible representation has recently received increasing attention and novel methods have been proposed [22], [23], [24], [25], [26], [27]. Differently from these approaches, we address compatibility by encouraging *stationarity* on the learned internal representation. The simple intuition is that stationarity allows features’ distribution not to change under time shift so that the current learned features are not conflicting with the old ones. In particular, our training methodology is based on two main concepts: (1) we use feature stationarity properties of classifiers whose parameters are not subject to learning; (2) we use the output of future/unseen classes to leave them a *reserved* representation space. The insight of reserving a representation space is that it prevents future classes from coming into conflict with already learned ones thereby further promoting stationarity. Both feature stationarity and space reservation are obtained by learning a surrogate classification task with a special classifier in which the weights are *fixed*. A very preliminary exploration of this complex subject was presented in [28], where we have shown that the performance of the Class-incremental Learning task (CiL) [29], [30] using fixed classifiers does not degrade with respect to the standard learned linear classifier.

Here, we address the different and distinguished problem of sequential learning of compatible features in an open-set verification/identification scenario. We argue that the stationary properties of the feature representation *emerged* in [28] are crucial for sequential learning of feature compatibility. We called our method Compatible Representations via Stationarity (CoReS).

In Sec. 2, we discuss the compatible learning problem in relation to the relevant areas of Class-incremental Learning and in Sec. 3, we highlight our contributions. Sec. 4, Sec. 5, and Sec. 6 present the details of the problem, the background, the motivation, and the proposed training procedure, respectively. In Sec. 7, we compare CoReS with state-of-the-art methods in a multi-model compatibility setting. Sec. 8 reports the ablation study and further improvements for the proposed method.

2 RELATED WORKS

Compatible Representation Learning. The term backward compatibility has been firstly introduced in [31] for *classification* tasks. They noted that even though machine learning models can increase on average their performance through the availability of more data, new classification outputs can be different from previously correct ones. As a consequence, the trust in machine learning systems is severely harmed by such errors. An illustrative example from [31] is over-the-air model updates in autonomous driving systems that change the user expected behavior of the car. Compatibility in classification has been further developed in [32], [33], [34] [35]. Although the general principle is the same, learning compatible *representation* models is substantially different

from learning compatible classifier models since in learning compatible classifiers, *no* constraints are directly imposed in the semantic distance of the feature representation.

Recent works on compatible representation learning [22], [23], [24], [25], [26], [27] underline how modern visual search systems often need to be upgraded with novel data. In particular, [24], [25], [26], [27] address the problem of compatible learning between two representation models. These works achieve compatibility by learning a *map* between the two representation models so that new and old feature vectors can be directly compared. The map in [24] is learned by a procedure consisting of three stages: adversarial learning for reconstruction, feature extraction and regression to jointly optimize the whole model. In [25] the map is learned through an autoencoder by minimizing the errors between the two representation spaces and the reconstruction errors. In [26] the learned map is a residual bottleneck transformation module trained by three different loss: classification loss, similarity loss between feature spaces, and, KL-divergence loss between the prototypes of the classifiers. In [27] the estimated map aligns the class prototypes between the models. To further encourage compatibility, the method also reduces intra-class variations for the new model. These methods do not completely prevents the cost of re-indexing since the learned maps require to be evaluated every time the dataset is upgraded and are therefore not suited to sequential learning and/or large gallery-set. For example, the ResNet-101 architecture is one order slower that the mapping proposed in [24], therefore when the size of the gallery increases by an order of magnitude it is equivalent to re-index the images.

Differently from these works, we leverage stationary features, thus avoiding learning specific space to space mappings for each previous upgraded representation model. The training strategy we propose learns a compatible representation to *all* the previous upgraded representations. The advantage is to completely avoid the cost of re-indexing and make the proposed method particularly suitable for sequential learning. Our work therefore shares the same goal of Backward Compatible Training (BCT) [22], [23]. The term “backward” refers to the explicit capability of achieving compatibility with all of the previously learned models. BCT takes advantage of an influence loss to achieve compatibility, where the old classifier is *fixed* during the learning with the novel data of the model and it cooperates with the new representation model. Cooperation is achieved by aligning the prototypes of the new classifier with the prototypes of the old fixed one. Although the idea is very promising, if the previously learned classifier does *not* sufficiently separate the learned features, the current classifier cannot improve this separation because it follows the previous one which can no longer be learned. Moreover, it can be noted that pairwise cooperation achieves sequential compatibility only indirectly through transitive compatibility (i.e., ϕ_3 is indirectly compatible with ϕ_1 since ϕ_3 is compatible with ϕ_2 that is compatible with ϕ_1). Since our method is not based on pairwise learning, it does not inherit previously wrong learned classifiers and it achieves direct compatibility, making it specifically suitable for sequential learning. BCT has been extended in [23] by taking into account small and large representation models for the query

and the gallery, respectively.

Compatibility from a broader perspective has been implicitly studied in [36], [37] in which representation similarity between two networks with identical architecture but trained from different initialization has been quantitatively evaluated.

Class-incremental Learning (CiL). CiL sequentially increases the number of classes to be learned by the model over time [29], [30], [38]. Although it might look similar to sequential learning of compatible features, the main focus of CiL is reducing catastrophic forgetting [39] (i.e., the tendency of a model to forget previously learned information upon learning new information). Compatible learning differs from CiL in two important aspects: (1) the new model is *not* required to be initialized as the old model and (2) the model has access to the *whole data* during the model upgrade. Thus, compatible feature representations are learned performing incremental multitask learning so that catastrophic forgetting has no effect on the final learned representation.

3 MAIN CONTRIBUTIONS

We summarize our main contributions as follows:

- 1) We propose a novel training procedure for learning compatible feature representation via stationarity.
- 2) We empirically verify in the open-set verification/identification problems (i.e. face recognition, person re-identification and image retrieval) that CoReS stationarity allows the sequential learning of compatible features without having to access to previously learned models and without learning space to space mappings.
- 3) We introduce novel criteria for comparing and evaluating compatible representation in sequential learning methods.
- 4) Our approach improves the current state-of-the-art in learning compatible features. The experimental evaluation that we performed includes single and sequential multi-model upgrading in growing large-scale training datasets.

4 PROBLEM STATEMENT AND EVALUATION METRICS

With reference to Fig. 1, we indicate with $\mathcal{G} = \{\mathbf{f}_i\}_{i=1}^N$ the gallery-set, where \mathbf{f}_i are the features extracted from the gallery-data, indicated as $I_G = \{\mathbf{x}_i\}_{i=1}^N$, and N is the number of elements of the two sets. The gallery-set \mathcal{G} can include classes or identities $\mathcal{Y} = \{y_1, y_2, \dots, y_N\}$ associated with the features. We have a representation model ϕ_{old} that transforms images \mathbf{x} into features, $\mathbf{f} = \phi_{\text{old}}(\mathbf{x})$, with $\mathbf{f} \in \mathbb{R}^d$ and where d is the dimension of the feature representation. The model ϕ_{old} is trained on the training-set \mathcal{T}_{old} . The feature vectors obtained by transforming the gallery-data I_G are typically used to perform search tasks through some distance $\text{dist} : \mathbb{R}^d \times \mathbb{R}^d \rightarrow \mathbb{R}_+$ to identify the closest features to a set of query images, indicated as I_Q . As new data \mathcal{X} become available, a new training-set $\mathcal{T}_{\text{new}} = \mathcal{T}_{\text{old}} \cup \mathcal{X}$ is created to improve the model ϕ_{old} . The new representation obtained from ϕ_{new} is different from ϕ_{old} .

To obtain the benefits of the new representation model ϕ_{new} , features that are in the gallery-set \mathcal{G} should be used directly, that is *without re-indexing* the original images I_G by ϕ_{new} . Equivalently, the already computed feature vectors from ϕ_{old} for these images should be used. Our goal is to design a training procedure to learn a new representation model ϕ_{new} so that any query image can be used to perform search tasks with features \mathcal{G} , without the need to compute $\phi_{\text{new}}(I_G)$. The resulting representation ϕ_{new} is then *compatible* with ϕ_{old} .

The problem extends to an arbitrary number of time steps T in which models are sequentially learned. As more data \mathcal{X}_t at time t is available, a new training-set \mathcal{T}_t is created to train the model ϕ_t , which is defined as follows:

$$\mathcal{T}_t = \mathcal{T}_{t-1} \cup \mathcal{X}_t \quad (1)$$

where \mathcal{T}_{t-1} is the training-set at step $t - 1$, with $t \in \{1, 2, \dots, T\}$.

4.1 Compatibility Evaluation

For the evaluation of feature compatibility, we refer to the criteria recently introduced in [22], that we briefly describe in the following.

Empirical Compatibility Criterion (ECC). A compatible representation model must be at least as good as the old one in clustering images from the same class and separating those from different classes. A new representation model ϕ_{new} is therefore compatible with an old representation model ϕ_{old} if:

$$\begin{aligned} \text{dist}(\phi_{\text{new}}(\mathbf{x}_i), \phi_{\text{old}}(\mathbf{x}_j)) &\leq \text{dist}(\phi_{\text{old}}(\mathbf{x}_i), \phi_{\text{old}}(\mathbf{x}_j)) \\ &\quad \forall (i, j) \in \{(i, j) \mid y_i = y_j\} \\ &\quad \text{and} \\ \text{dist}(\phi_{\text{new}}(\mathbf{x}_i), \phi_{\text{old}}(\mathbf{x}_j)) &\geq \text{dist}(\phi_{\text{old}}(\mathbf{x}_i), \phi_{\text{old}}(\mathbf{x}_j)) \\ &\quad \forall (i, j) \in \{(i, j) \mid y_i \neq y_j\}, \end{aligned} \quad (2)$$

where $\text{dist}(\cdot, \cdot)$ is a distance in feature space. Since it constrains all pairs of samples, Eq. 2 is therefore considered inadequate for true characterization and it is relaxed to the following *Empirical Compatibility Criterion*:

$$M(\phi_{\text{new}}^Q, \phi_{\text{old}}^G) > M(\phi_{\text{old}}^Q, \phi_{\text{old}}^G), \quad (3)$$

where M is an evaluation metric based on $\text{dist}(\cdot, \cdot)$. The notation $M(\phi_{\text{new}}^Q, \phi_{\text{old}}^G)$ underlines that the updated model ϕ_{new} is used to extract the feature vectors Q from the query-set images I_Q , while the old model ϕ_{old} is used to extract the features \mathcal{G} from the gallery-data I_G , and that the metric M is used to evaluate the performance from the two feature sets. This performance value is referred to as *cross-test*, as it evaluates the case in which the query is extracted with the new model while the gallery with the old one. The term $M(\phi_{\text{old}}^Q, \phi_{\text{old}}^G)$ is referred to as *self-test* as it evaluates the case in which both query and gallery features are extracted with ϕ_{old} . The underlying intuition is that if the performance of using the feature vectors obtained with the previous models with the upgraded query features (i.e., cross-test) is better than the performance with the features extracted from the old model (i.e., self-test), then the system is learning compatible representations. That is, the new training data improves

the representation without breaking the compatibility with the previous one.

Update Gain. To evaluate the relative improvement gained by a new learned compatible representation with respect to an old one, [22] further defines the following *Update Gain*:

$$\Gamma(\phi_{\text{new}}^{\mathcal{Q}}, \phi_{\text{old}}^{\mathcal{G}}) = \frac{M(\phi_{\text{new}}^{\mathcal{Q}}, \phi_{\text{old}}^{\mathcal{G}}) - M(\phi_{\text{old}}^{\mathcal{Q}}, \phi_{\text{old}}^{\mathcal{G}})}{M(\tilde{\phi}_{\text{new}}^{\mathcal{Q}}, \tilde{\phi}_{\text{new}}^{\mathcal{G}}) - M(\phi_{\text{old}}^{\mathcal{Q}}, \phi_{\text{old}}^{\mathcal{G}})}, \quad (4)$$

where $\tilde{\phi}_{\text{new}}^{(\cdot)}$ is the model learned according to the *joint training and re-indexing* strategy which can be considered as the upper bound of the best achievable performance. Eq. 4 quantifies the gain produced by the learned compatible representation with respect to the non-compatible one learned by the upper bound.

5 MOTIVATIONS AND BACKGROUND

We now focus on the motivations underlying our training procedure and briefly recall the required technical background to formulate our method.

Training from Scratch. When Neural Network models are trained from a model in which weights are randomly initialized, their internal feature representation is subject to a substantial variation during learning. It is well known that: (1) features can be learned reliably in *different* architectures when trained on a common dataset and (2) the subspaces so trained are common to multiple different networks, however, as shown in [36], [37], the specific learned *subspace basis vectors* are substantially different. Therefore, training CNNs from scratch with randomly initialized weights does *not* provide similar representations in terms of subspace geometry. This result *excludes* compatibility between two independently trained representation models.

Training from a Previously Learned Model. The alternative training procedure that would seem more favorable to compatibility is learning with *Incremental Fine-Tuning* (IFT) from a model in which weights are initialized from the previously learned model. However, and perhaps counter-intuitively, this does not help to obtain similar subspace representation geometry suited for compatibility. With reference to Fig. 2, we provide direct evidence of this intrinsic aspect of feature learning (more in Sec. 7.6). In this toy problem, we trained on a subset of the MNIST dataset the LeNet++ architecture in *two-dimensional* representation space [40]. This is achieved by setting the output size of the last hidden layer to two (no dimensionality reduction techniques are applied). The LeNet++ network is a modification of the LeNet [41] to a deeper and wider network. We follow standard practice in feature learning, classifier weights and biases are unit normalized and set to zero, respectively, to encourage learning cosine distance between features [42], [43] and cross-entropy loss with softmax output is minimized. For the sake of clarity, we grow the training set \mathcal{T}_{new} by one single class: from five classes to six as shown in Fig. 2(a) and Fig. 2(b), respectively. The same characterization holds for any number of classes and feature space dimension.

As can be noticed from the figures, changes in the extracted features (colored point clouds) are due to the inclusion of the novel class. Specifically, as the new class (brown) is included in the training-set and the representation fine-tuned, the features of the old classes (red, orange,

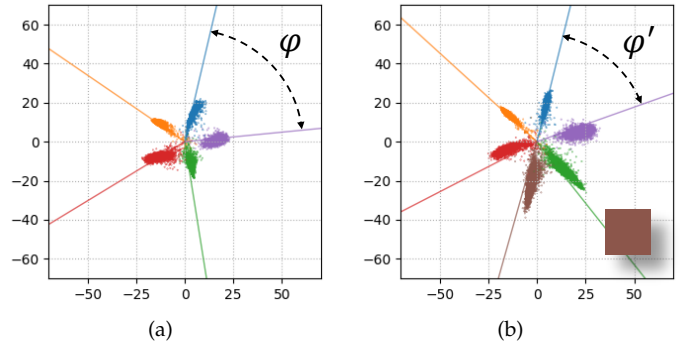


Fig. 2. Training the LeNet++ network initialized from a previously learned model (i.e., fine-tuning) using the MNIST dataset. To visualize features, the output size of the last hidden layer is reduced to two. Colored cloud points are features from the test-set and colored lines represent classifier prototypes. (a): Learning is performed with a training-set \mathcal{T}_{old} consisting of the first five classes of the MNIST dataset. (b): Learning by fine-tuning $\mathcal{T}_{\text{new}} = \mathcal{T}_{\text{old}} \cup \{\text{brown-class-data}\}$. The new class determines the effect of varying the spatial configuration of the representation (i.e., angles between class features change). As an example in the figure $\varphi \neq \varphi'$.

blue, purple, and green) change their spatial configuration to accommodate the novel class. This is due to the fact that linear classifiers maximize inter-class distance to better discriminate between classes [40]. The consequence is that direct comparison between old and new features, based for example on the cosine distance, is not guaranteed to be determined by the same angle (i.e., $\varphi \neq \varphi'$). To limit the spatial variation effect of the features, and therefore achieve compatibility, our approach learns stationary features according to the fixed classifiers introduced in [44] that we briefly recall in the next subsection.

5.1 Learning Stationary Features

As shown in the two-dimensional case of Fig. 2, a standard learned linear classifier based on softmax and optimized with cross-entropy tends to split the available space into equiangular regions (similar to N -sided regular polygons) in which features are well separated. Recently in [44] it has been shown that this behavior can be reproduced with non-trainable (i.e., *fixed*) linear classifiers to further add stationarity to learned features. This is achieved by setting classifier prototype vectors w_i to values taken from the coordinate vertices of a specific *regular polytope* and leaving them not subject to learning. Regular polytopes are the generalized analog in any number of dimensions of N -sided regular polygons. As the parameters w_i are set as non-trainable (i.e., *fixed*), *only* the feature vector directions align toward the classifier weight vector directions achieving *stationarity* [44]. By fixing the weights, the trainable classifier is basically superseded by previous layers. Therefore, differently from the works [24], [25], [26], [27], that learn external learnable maps between representation spaces, in our method the functional complexity of learning a compatible representation is demanded to internal layers of the neural network.

6 COMPATIBILITY VIA STATIONARITY

Fig. 3 shows our training procedure in two-dimensional representation space leveraging the structure of the fixed

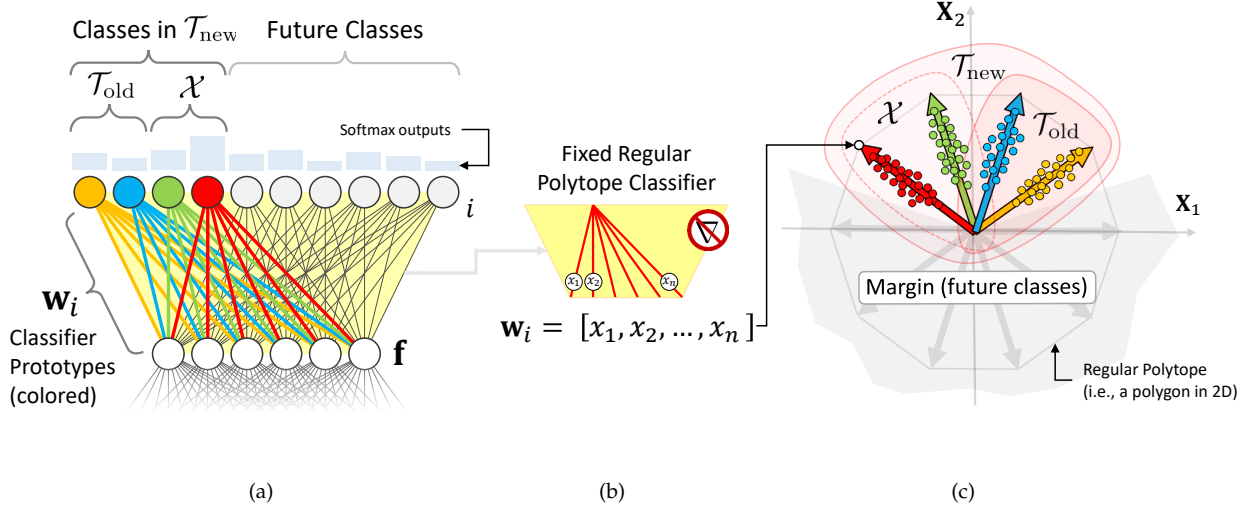


Fig. 3. Overview of CoReS. (a): The regular-polytope classifier in a neural network architecture with highlighted the datasets \mathcal{T}_{old} , \mathcal{T}_{new} , the new available data \mathcal{X} , the classifier prototypes $\{\mathbf{w}_i\}$, the future classifier outputs, the softmax outputs, and the feature \mathbf{f} . (b): A single fixed classifier prototype highlighted from Fig.(a). The prototype coordinates x_1, x_2, \dots, x_n are set to coordinate vertices of a regular polytope. (c): The two-dimensional illustrative representation space generated by the regular polytope classifier. The gray region is the margin region imposed by the outputs of the future/unseen classes for which no samples are available. The region is defined around the prototypes of the future classes (gray arrows). The colored point clouds show the learned features along their respective stationary classifier prototypes. Learned features are pushed out from the margin.

classifier in which future class outputs are added without samples. Compatible representation learning is achieved by sequentially training on \mathcal{T}_{old} and \mathcal{T}_{new} as formulated in Sec. 4. For the sake of clarity, we illustrated both \mathcal{T}_{old} and the new data \mathcal{X} having two classes each. The resulting training dataset \mathcal{T}_{new} to upgrade the compatible representation has four classes and in Fig. 3(c) it is shown applied to a 2D regular polytope (i.e., a 10-sided polygon).

We use the so called d -Simplex regular polytope fixed classifier in which class prototypes are near to all others (i.e., the simplex is the generalization of the triangle to higher dimensions) [45]. The topology of the simplex allows to make no assumptions about the semantic similarity between previously learned classes and future/unseen ones. In particular the prototypes for the fixed classifier can be computed as: $\{\mathbf{w}_i\} = \{e_1, e_2, \dots, e_{d-1}, \alpha \sum_{i=1}^{d-1} e_i\}$, where $\alpha = \frac{1-\sqrt{d+1}}{d}$ and e_i with $i \in \{1, 2, \dots, d-1\}$ denotes the standard basis in \mathbb{R}^{d-1} . Learning with CoReS proceeds by instantiating the fixed classifier and optimizing the following loss:

$$\mathcal{L}_t = -\frac{1}{N_b} \sum_{\mathbf{x} \in \mathcal{T}_t} \log \left(\frac{e^{\mathbf{w}_{y_i}^\top \phi(\mathbf{x})}}{\sum_{j=1}^{|\mathcal{T}_t|} e^{\mathbf{w}_j^\top \phi(\mathbf{x})} + \sum_{j=|\mathcal{T}_t|+1}^{K_p} e^{\mathbf{w}_j^\top \phi(\mathbf{x})}} \right), \quad (5)$$

where \mathcal{T}_t is the training set at time t as defined in Eq. 1, ϕ is the representation model, N_b is the number of elements in a mini-batch, y_i is the label of the class that supervises the classifier output and K_p is the number of classifier outputs. For $K_p - |\mathcal{T}_t|$ outputs, no training input samples and output labels are available at time t . The false positive responses generated by the second term of the denominator in Eq. 5 allow reserving feature space for future usage so that every assimilated class a time t does not cause feature conflict effects with respect to the already learned classes.

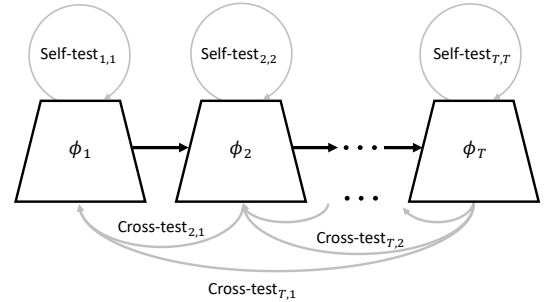


Fig. 4. Multi-model Empirical Compatibility Criterion (Eq. 6). The representation models ϕ_i with $i = 1, 2, \dots, T$ are sequentially learned (black arrows). The cross-tests involve pairs of different models, while the self-tests involve the same models (gray arrows).

Because the number of classes K_p equal to the number of vertices of the d -Simplex fixed classifier: $K_p = d + 1$, the representation dimensionality grows linearly with respect to the number of classes. However, this does not affect the training speed or excessive memory consumption since the fixed parameters of the classifier do not need to be updated by back-propagation [44], [46].

6.1 Sequential Compatibility Criterion

When representation models are sequentially learned in T steps, we generalized Eq. 3 to the following Multi-model Empirical Compatibility Criterion:

$$M(\phi_i^Q, \phi_j^G) > M(\phi_j^Q, \phi_i^G), \quad \text{with } i > j, \quad (6)$$

where the time steps $i, j \in \{1, 2, \dots, T\}$ refer to two different models such that ϕ_j is learned before ϕ_i . The model ϕ_i is compatible with the model ϕ_j , when the cross-test between ϕ_i and ϕ_j is greater than the self-test of the model ϕ_j . Fig. 4 illustrates the Multi-model Empirical Compatibility Criterion, where $\{\phi_1, \phi_2, \dots, \phi_T\}$ are the representation models,

the black arrows indicate the sequence of models and the gray arrows represent the compatibility tests. The cross-tests involve a pair of models, while the self-tests a single one. Eq. 6 allows defining the *compatibility matrix*, in which rows represent new models and columns represent old models. The compatibility matrix C is a square triangular matrix defined as:

$$C_{i,j} = \begin{cases} M(\phi_i^Q, \phi_j^G) & \text{if } i > j \\ M(\phi_j^Q, \phi_j^G) & \text{if } i = j \end{cases} \quad (7)$$

The value $C_{i,j}$ represents the evaluation metric M of model i to model j . Elements on the main diagonal, $i = j$, represent the *self-test*, while the elements off-diagonal, $i > j$, represent the *cross-test*. The compatibility matrix of Eq. 7 has a similar mathematical formulation, but with the purpose of compatibility, to the accuracy matrix $R_{i,j}$ ² defined in [47] to quantify forward and backward transfer in CL.

Besides monitoring compatibility performance across tasks, Eq. 7 is used to provide a single overall scalar metric to quantify the sequential compatibility. We define the Average Compatibility (AC) as the number of times that Eq. 7 is verified divided by the total number of times it could occur, as follows:

$$AC = \frac{2}{T(T-1)} \sum_{1 \leq j < i \leq T} \mathbb{1}(M(\phi_i^Q, \phi_j^G) > M(\phi_j^Q, \phi_j^G)), \quad (8)$$

where $\mathbb{1}(\cdot)$ denotes the indicator function. This metric is also independent of the number of the learning steps T .

We further define the average of the entries of the compatibility matrix as:

$$AM = \frac{2}{T(T+1)} \sum_{1 \leq j \leq i \leq T} C_{i,j}. \quad (9)$$

This metric captures the overall accuracy M achieved under compatible training.

7 EXPERIMENTAL RESULTS

We evaluate our approach on different datasets and network architectures, comparing it with several baselines and the current state-of-the-art method. In the first part of this section, we evaluate the proposed approach in a single model upgrade on the CIFAR datasets and, in the second part, the evaluation is performed in sequential model updating. Furthermore, we evaluate CoReS in the more challenging task of face verification and (body) re-identification with more sophisticated network architectures and datasets. We also report a qualitative analysis of the feature space learned by CoReS and other methods discussing the importance of stationary features to achieve compatibility. The ablation study is presented in Sec. 8.

7.1 Baseline Methods

We compare CoReS with the following baselines: *Naive*, *Incremental Fine-Tuning* (IFT), *Learning without Forgetting* (LwF) [48] and *Backward Compatible Training* (BCT) [22]. The Naive approach trains the model ϕ_{new} to be compatible with ϕ_{old} , minimizing some distance between the

features computed on the same images. This is imposed using each image \mathcal{T}_{old} used to train ϕ_{old} with an auxiliary loss $\mathcal{L}_{\text{dist}}(\phi_{\text{new}})$ training the new representation model, as $\phi_{\text{new}} = \arg \min_{\phi} \mathcal{L}(\phi, \mathcal{T}_{\text{new}}) + \lambda \mathcal{L}_{\text{dist}}(\phi)$, where $\mathcal{L}_{\text{dist}}(\phi) = \frac{1}{|\mathcal{T}_{\text{old}}|} \sum_{\mathbf{x} \in \mathcal{T}_{\text{old}}} \text{dist}(\phi(\mathbf{x}), \phi_{\text{old}}(\mathbf{x}))$, \mathcal{L} is the standard cross-entropy loss and the scalar λ balances the two losses. The Naive baseline, is instantiated with the Euclidean distance ℓ^2 and is referred as $\phi_{\text{new-}\ell^2}$. Note that ϕ_{old} it is not subject to learning. Except for IFT the baselines are based on the publicly available implementations³ of [22]. As a reference, we also report the performance of the the upper bound obtained by joint training and re-indexing. The upper bound is also used to evaluate the Update Gain of Eq. 4.

7.2 Benchmarks

To assess the effectiveness of CoReS, we evaluate our approach on different benchmarks and under the 1:1 and the 1:N search problems in an open-set context [49]. In the open-set evaluation protocol the classes in the training-set are different from the classes in the test-set. The open-set evaluation is also particularly valuable as it allows using a gallery with a constant number of elements. The alternative closed-set evaluation would require evaluating Eq. 3 and Eq. 6 with an increasing number of images at each upgrade. Consequently, the evaluation would depend on an increasing number of elements that would make it more difficult to define. We briefly report the details of each benchmark and describe the involved evaluation metrics.

CIFAR-100 and CIFAR-10. The CIFAR-100 and CIFAR-10 datasets consist of 60000 32×32 RGB images in 100 and 10 classes, respectively [50]. There are 50000 training images and 10000 test images. As CIFAR-100 and CIFAR-10 contain a set of disjoint classes, we use the CIFAR-100 to build training-sets to upgrade the representation models and CIFAR-10 as the test set to evaluate compatibility. In particular, we focus on the verification protocol in which given a pair of images of unseen classes taken from the CIFAR-10 dataset, the task is to decide whether the images contain the same class or not. At test time, we randomly generate from 6000 verification pairs from the test-set, composed by 3000 positive pairs and 3000 negative ones. The verification protocol is based on the cosine distance between the two feature vectors.

CASIA-WebFace and Labeled Face in the Wild (LFW). The CASIA-WebFace dataset [51] is composed by 10575 subjects and 494414 RGB face images. The LFW benchmark [52] contains 13233 target face images of 5749 different subjects. Of these, 1680 people have two or more images in the database, while the remaining 4069 people have just a single image in the database. The two datasets do not have common classes and therefore we use CASIA-WebFace to build training datasets to upgrade the representation models and LFW to perform open-set face verification to evaluate compatibility.

Market1501. Market1501 [53] dataset contains 1501 identities divided in 751 training identities and 750 test identities. The two sets do not contain common classes and therefore he dataset is suited to perform open-set 1:N identification to evaluate compatibility. Images of each identity are captured

2. The matrix $R_{i,j}$ in [47] reports the test classification accuracy of the model on task j after learning the task i .

3. <https://github.com/YantaoShen/openBCT>

TABLE 1

Two-model compatibility. Experiments based on the 1:1 verification (M) on CIFAR-10. The two models are learned on the CIFAR-100, with 50% and 100% of data, respectively. The ‘‘Comparison Pair’’ $(\phi_{(\cdot)}, \phi_{(\cdot)})$ indicates the representation models evaluated for compatibility. $\phi_{\text{new-X}}$ indicates a representation with ϕ_{old} learned with the specific method X .

COMPARISON PAIR	M	ECC	Γ (%)	ABSOLUTE GAIN
$(\phi_{\text{old}}, \phi_{\text{old}})$ (Lower Bound)	0.60	–	–	–
$(\phi_{\text{new-}\ell^2}, \phi_{\text{old}})$	0.35	×	–	–
$(\phi_{\text{new-IFT}}, \phi_{\text{old}})$	0.57	×	–	–
$(\phi_{\text{new-LwF}}, \phi_{\text{old}})$	0.59	×	–	–
$(\phi_{\text{new-BCT}}, \phi_{\text{old}})$	0.60	✓	5.9	0.20
$(\phi_{\text{new-CoReS}}, \phi_{\text{old}})$ (Ours)	0.61	✓	21.3	1.05
$(\tilde{\phi}_{\text{new}}, \tilde{\phi}_{\text{new}})$ (Upper bound)	0.65	–	–	0.49

by at most six cameras and each identity is captured by at least two cameras so that cross-camera search can be performed. For 1:N identification, a set of templates is first indexed as the gallery-set. Then each template in the query-set is used to search against the indexed templates. The quality metrics for this protocol is mean Average Precision (mAP).

7.3 Compatibility Evaluation on CIFAR-100/10

To maximize usage of available data and to ensure reproducibility, we use CIFAR-100 to sample a growing training dataset to sequentially upgrade the representation model and leverage CIFAR-10 as test-set. To evaluate the performance in sequential model upgrading, we split the CIFAR-100 dataset accordingly. The growing training-set is increased by $\lfloor K_{\text{dataset}}/T \rfloor$ classes at each step, where K_{dataset} is the total number of classes in the dataset (e.g., 100 in CIFAR-100).

For a fair comparison, CoReS and the other baseline methods are evaluated on the same architecture. We used the recent SENet-18 architecture [54] adapted⁴ to the CIFAR 32×32 input size. When not otherwise specified, we initialize the model with the same set of random weights, i.e., using the same random seed, every time the model is upgraded. The ablation study of this parameter is performed and discussed in Sec. 8.3. We set the number of output nodes of the fixed classifier to $K_p = 100$ and therefore the feature space is 99-dimensional. The worst case analysis scenario of Class-incremental Learning with a larger number of output nodes has been already evaluated in [28] and therefore not further discussed. Optimization is obtained using SGD with learning rate of 0.1, momentum of 0.9, and weight decay of $5 \cdot 10^{-4}$. The batch size is set to 128. The training is terminated after 100 epochs and the learning rate is scheduled to decrease to 0.01 after 70 epochs.

In this scenario, in which the representation model is upgraded once, we first train a representation model ϕ_{old} on 50% of the classes of CIFAR-100 and subsequently the representation is upgraded using the 100%. The compatibility of the pair of models $(\phi_{\text{new}}, \phi_{\text{old}})$ obtained with each

baseline is evaluated according to the Empirical Compatibility Criterion (Eq. 3) and the Update Gain (Eq. 4) as described in Sec. 4.1. Tab. 1 shows that only BCT and CoReS satisfy Eq. 3. Both $\phi_{\text{new-BCT}}$ and $\phi_{\text{new-CoReS}}$ learn a representation ϕ_{new} compatible with the representation ϕ_{old} , and CoReS achieves higher Update Gain with respect to BCT. Naive, IFT, and LwF perform worse with respect to using ϕ_{old} . Reasons are to be found in the fact that the constraints imposed by these methods do not substantially influence the stationarity of the learned representation.

We evaluate the compatibility between three models trained sequentially. We train ϕ_1 on the 33% of training-set, ϕ_2 on the 66% and ϕ_3 on the 100% of CIFAR-100. To facilitate the comparison, the results shown in Figs. 5(a)-(e) are presented according to the compatibility matrix defined in Eq. 7 in which not compatible models are highlighted in red. Consistent with the previous experiment, BCT and CoReS achieve higher compatibility with respect to the other baselines. CoReS achieves nearly full compatibility as the model ϕ_3 is compatible with ϕ_1 , and the model ϕ_2 is nearly compatible with ϕ_3 (i.e., self and cross tests differ by 0.015). In Tab. 2 the comparison of the Update Gain of the learned representations shows that CoReS achieves a substantial higher Update Gain of 54.7 with respect to BCT that achieves 52. Possible reasons of the better performance of CoReS may be connected to the fact that in BCT the compatibility of the last model ϕ_3 with ϕ_1 is learned indirectly without any relationships with ϕ_1 . While the compatibility of the representation learned by CoReS is jointly encouraged to all the models through the common fixed reference specified by the classifier prototypes.

Figs. 5(f)-(g) and Figs. 5(h)-(i) show the comparison between BCT and CoReS in the case of five and ten-model compatibility, respectively. As the number of model upgrade increases, CoReS achieves higher compatibility and largely outperforms BCT. In the case of five-model compatibility, for example, CoReS only fails for the pair (ϕ_3, ϕ_1) . In the more challenging case of ten-model compatibility, CoReS succeeds in achieving compatibility between pairs of representation models 23 times, while BCT 5 times, scoring an AC (Eq. 8) values of 0.51 and 0.11 respectively.

TABLE 2

Three-model compatibility. Experiments based on the 1:1 verification (M) on CIFAR-10. The three models are learned on the CIFAR-100, with 33%, 66% and 100% of data, respectively. The ‘‘Comparison Pair’’ (ϕ_i, ϕ_j) indicates the representation models evaluated for compatibility.

COMPARISON PAIR	CoReS (Ours)			BCT		
	M	ECC	Γ (%)	M	ECC	Γ (%)
(ϕ_1, ϕ_1)	0.59	–	–	0.59	–	–
(ϕ_2, ϕ_1)	0.61	✓	54.7	0.59	✓	52
(ϕ_3, ϕ_1)	0.60	✓	18.5	0.58	×	–
(ϕ_2, ϕ_2)	0.63	–	–	0.61	–	–
(ϕ_3, ϕ_2)	0.61	×	–	0.59	×	–
(ϕ_3, ϕ_3)	0.65	–	–	0.64	–	–

4. Code source for SENet-18 <https://github.com/kuangliu/pytorch-cifar>

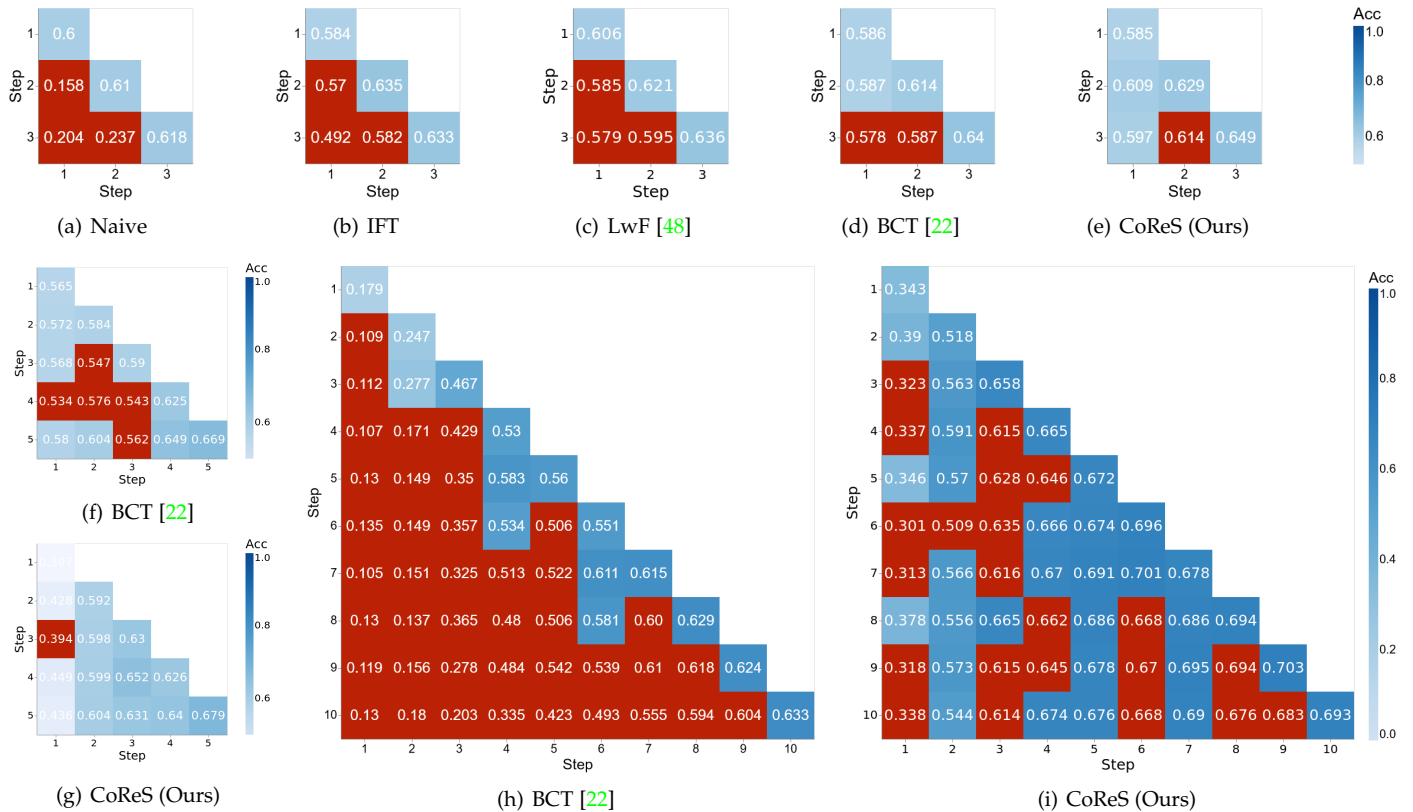


Fig. 5. Compatibility matrices based on the 1:1 verification accuracy on CIFAR-10. Models are sequentially learned on CIFAR-100 with: (a)-(e): 33%, 66%, 100% of data; (f) and (g): 20%, 40%, 60%, 80%, 100% of data; (h) and (i): 10%, 20%, ..., 100% of data. Evaluation is performed on CIFAR-10. Models not achieving compatibility are highlighted in red. Diagonal elements report the self-test accuracy and off-diagonal elements report the cross-test accuracy (See Eq. 7 for the details). Compared methods are indicated in the sub-captions.

7.4 Compatibility evaluation on CASIA-WebFace/LFW

We evaluate the compatible representation learned by our approach on the challenging task of face verification by building multiple datasets from the CASIA-WebFace to sequentially upgrade the models. The compatibility of the upgraded models are evaluated on the LFW benchmark according to a verification task. We use the ResNet50 [55] as model architecture with input size of 112×112 . For every upgrade, training is terminated after 120 epochs, the learning rate is initialized to 0.1 and decreased to 0.01, 0.001, and 0.0001 at epoch 30, 60, 90 respectively and the batch size is set to 1024. To train the representation models we used 4 NVIDIA Tesla A-100 GPUs. Tab. 3 reports the results for both CoReS and BCT when the model is trained with 50% and 100% of the dataset. As can be noticed, both BCT

and CoReS achieve comparable compatibility performances with CoReS reporting slightly higher Update Gain Γ . The different results with respect to the CIFAR-10/100 evaluation of the previous section are mostly due to the fact that the 50% percent of a large dataset like the CASIA-WebFace allows directly learn reasonably good features to represent the remaining 50% of the data. Another reason may be due to the fact that in two-model compatibility BCT does not suffer from the transitive learning limit, thus learning directly the compatibility using the available previous model.

We further evaluate our approach in multi-model scenarios with three, four, five and ten-model sequential step upgrade. Results are summarized in Fig. 6 according to the AC and the AM metrics of Eq. 8 and Eq. 9, respectively. Fig. 6(a) points out the difference in the achieved compatibility representations between CoReS and BCT. In particular, our method achieves full compatibility, that is, $AC = 1$, when the model is trained for two, three, four, and five step, and 0.57 for the challenging 10-model compatibility setting. Fig. 6(b) shows the verification accuracy AM decreasing favorably for CoReS. Fig. 6(c) and Fig. 6(d) show the compatibility matrices for the 5-model compatibility learning setting of BCT and CoReS, respectively. In general, Fig. 6 shows not only that the results are consistent with the CIFAR ones, but that CoReS significantly improves compatible learning performance by a large margin also in face verification. We obtain a 49% increase (i.e., from the 0.09 of BCT to the 0.58 of CoReS) in measuring the AC , which is a 544% relative

TABLE 3

Two-model compatibility on LFW dataset. Experiments are based on the 1:1 verification (M). The two models are learned on the 50% and 100% of the data, respectively.

COMPARISON PAIR	CoReS (Ours)			BCT		
	M	ECC	Γ (%)	M	ECC	Γ (%)
(ϕ_{old}, ϕ_{old})	0.90	—	—	0.91	—	—
(ϕ_{new}, ϕ_{old})	0.91	✓	0.32	0.91	✓	0.29
(ϕ_{new}, ϕ_{new})	0.92	—	—	0.91	—	—

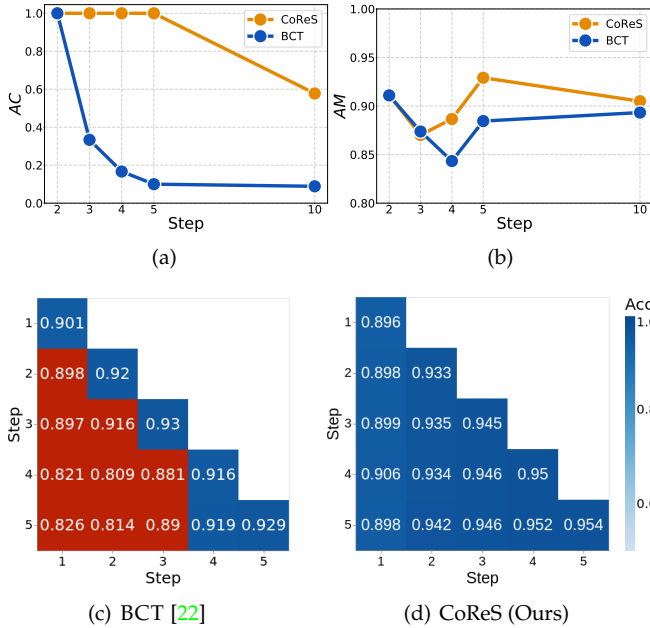


Fig. 6. LFW Face Verification results in sequential two, three, four, five, and ten-model compatibility. The compatible feature models are trained on a growing training dataset sampled from CASIA-WebFace. (a) The average compatibility AC score of Eq. 8 and (b) the average verification accuracy AM of Eq. 9 as the number of learning steps increases. Orange and blue colored curves indicate CoReS and BCT, respectively. (c) and (d) are the compatibility matrices of the five-models compatibility for BCT and CoReS, respectively.

improvement over previous state-of-the-art.

7.5 Compatibility evaluation on Market1501

In order to diversify the training data, we finally validate CoReS on the person re-identification task (ReID) using the Market1501 dataset. Differently from face data, ReID data typically include severe occlusion and pose variation. Following [56], we adopt a pre-trained ResNet101 [55] as feature extractor and Adam [57] as optimizer. We train the models for 25 epochs at each upgrade, with a initial learning rate of $3 \cdot 10^{-4}$, that is decreased to $3 \cdot 10^{-5}$ after 20 epochs. The mean Average Precision (mAP) is used as the accuracy metric M in Eqs. 3, 6, 7, 8, and 9. Tab. 4 summarizes the two and three-model compatibility evaluation we performed. As evidenced by the table, CoReS obtain full compatibility, i.e., $AC = 1$, in both two and three-model compatibility and an higher AM . Contrarily, in BCT the AC decreases = 0.3,

TABLE 4
Two and Three-model compatibility on Market1501 dataset. Experiments are based on the 1:N search problem using mAP as evaluation metric M . We report AC (Eq. 8) and AM (Eq. 9) for each configuration.

Method	#Steps	AC	AM
CoReS	2	1.0	0.57
	3	1.0	0.51
BCT	2	1.0	0.49
	3	0.3	0.50

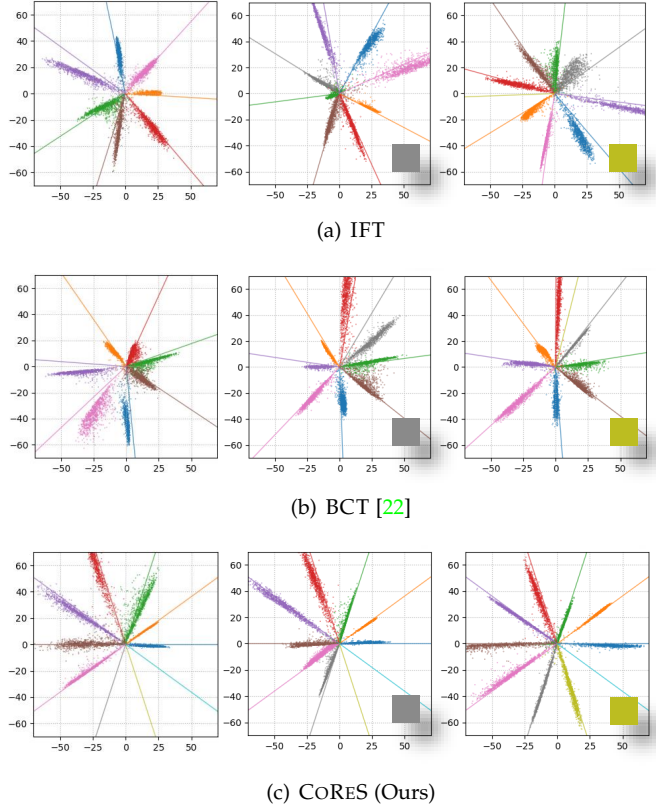


Fig. 7. Three-model compatibility with one class per step. Learning is performed using the MNIST dataset and the number of the outputs of the last hidden layer is reduced to two (i.e., features are two-dimensional). Cloud points are features from the test-set and lines represent classifier prototypes. Three different approaches are shown: (a): IFT, (b): BCT [22] and (c): CoReS.

when the models are sequentially upgraded three times. Although the data are significantly different, the results are nevertheless consistent with the experiments of the previous sections. Our method seems to have the explicit advantage of not relying on the previously learned model and to encourage compatibility in a global way. The positive and consistent results obtained in different data sets confirm the wide and practical applicability of CoReS in several visual research tasks.

7.6 Qualitative Results

To clarify the differences between the evaluated methods, we report qualitative results to obtain some intuitions about their behaviors. Fig. 7 shows the evolution of the learned representations with models trained sequentially with the training set \mathcal{T}_{new} grown by a single class per upgrade step, from seven classes to eight and successively to nine. We used the same training settings used to obtain the results of Fig. 2 for the MNIST dataset example. In particular, Fig. 7(a), Fig. 7(b), and Fig. 7(c) shows the evolution of IFT, BCT [22], and CoReS approaches, respectively. As it can be noticed, each novel class learned by IFT significantly and unpredictably changes the spatial configuration of the representation with respect to the previously learned models. No one of the class features and the relative classifier prototypes (shown as colored lines) remain close to the previous model. This is due to the fact that IFT has no

mechanism to prevent the re-arrangement of the features when novel information is assimilated. BCT keeps the representation reasonably stationary since it constrains the solution towards the previous learned classifier, however, variations to accommodate novel classes are evident. The olive class features, shown when learning from the eight to the nine class, are not as discriminative as the other classes, since they remained close to the origin. Differently from the others, features learned by CoReS remain accurately aligned to the 10-sided polygon classifier prototypes, thus avoiding the effect of varying the spatial configuration of the representation and thus compatibility.

8 ABLATION STUDIES

As CoReS is a single building block method, ablation study consists mostly in hyperparameters tuning. In the following subsections, we conduct extensive experiments to determine which factors contribute the most to the performance of our training procedure. In Sec. 8.1, we study how the number of epochs affects learning compatible representations. In Sec. 8.2 we discuss an extension of our training procedure to select the epoch at which the best model was learned based on our Multi-model ECC of Eq. 6. We also evaluate the effects of: (1) the model initialization of Sec. 8.3, with both random weights and by fine-tuning starting from the previously learned model, (2) different class sequence order in Sec. 8.4, (3) different architectures in Sec. 8.5 and (4) changing architecture between model upgrades Sec. 8.5.1. Ablation study of CoReS is performed on the verification task on the dataset CIFAR-100/10 as it is one of the more challenging for this problem and the faster to train.

8.1 Number of Epochs

To verify how the number of epochs affects each learned model in the final performance, we report the AC and the AM values of the 10-model sequence evaluated in the CIFAR-100/10 experiment in which models are learned sequentially with 30, 70, 100, 200 and 350 epochs at each upgrading step. The case of 100 epochs is already shown in Fig. 5(i) and it is included here for completeness. In this evaluation, we slightly modified the implementation details described in Sec. 7.3 to adapt the scheduling policy of the learning rate to the different numbers of epochs. We change the scheduling of the learning rate as follows: no scheduling for the 30 epochs case; decreased to 0.1 at 50-th epoch for 70 epochs scenario; decreased to 0.1, 0.01 at epochs 70, 140 respectively when the epochs are set to 200; decreased to 0.1, 0.01 at epochs 150, 250 respectively when the model is trained for 350 epochs per time step. Fig. 8 shows the results of the training for the selected number of epochs. Specifically, Fig. 8(a) reports the AC of Eq. 8 and Fig. 8(b) the AM of Eq. 9, respectively. The two indicators provide a concise summary of how the number of epochs contribute to the compatibility performance. As evidenced by the solid lines, AM increases with increasing epochs while AC decreases, showing, as expect, a clear trade-off between compatibility and verification accuracy. A reasonable balance, which is the one we used in this paper for the experiments, is around 100 epochs.

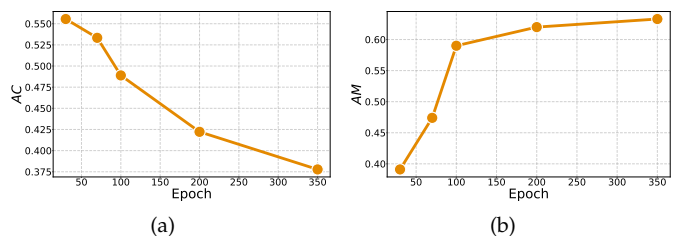


Fig. 8. Verification performance of CoReS evaluated on the CIFAR-100/10 data as the number of epochs increases. The model is trained for 30, 70, 100, 200, 350 epochs for each upgrade. (a) and (b) show the AC (Eq. 8) and the AM (Eq. 9) values, respectively.

8.2 Compatibility based Model Selection

At each upgrade, the sequential growing of the training-set with respect to a given and fixed gallery causes a change in the distribution between the training and the testing data which can be regarded as a form of dataset shift [58]. Under this learning condition, the distribution of the training-set and the gallery-set continuously change over time and *adaptive learning* strategies can alleviate the challenges of sequential learning by reacting to the shift. In the following, instead of learning for a fixed number of epochs, we provide experiments on whether CoReS can exploit previous learned models to better capture the trade-off existing between verification accuracy and compatibility. We exploit this learning context and provide a simple adaptive strategy based on the following assumptions: (1) drift is occurring *gradually* such that the density ratio of the marginal distribution before and after the upgrade is close to uniform [59] and (2) there is a set of data $\hat{\mathcal{G}}$ available that is an i.i.d. sample of the gallery-set data \mathcal{G} (i.e., a split following the same distribution). Under these assumptions, it is possible to adapt the training procedure to the dataset shift according to standard model selection techniques, such as cross-validation [60]. We propose a model selection strategy based on Eq. 6 to directly capture the underlying compatibility relation between previously learned models.

During the training phase of a model ϕ_i with the sequential training-set \mathcal{T}_i with $i \in \{1, 2, \dots, T\}$, a model is learned at each epoch for a total of N_e epochs. We search a model achieving the highest verification accuracy (i.e., the self-test) among the models satisfying the compatibility criterion of Eq. 6 with respect to the previous model. More formally this search problem is formulated as follows:

$$\phi^* = \arg \max_{n=1,2,\dots,N_e} M_n(\phi_i^{\mathcal{Q}}, \phi_i^{\hat{\mathcal{G}}}) \quad (10)$$

$$\text{s. t.} \quad M_n(\phi_i^{\mathcal{Q}}, \phi_j^{\hat{\mathcal{G}}}) > M_n(\phi_j^{\mathcal{Q}}, \phi_j^{\hat{\mathcal{G}}}) \quad (11)$$

$$\text{with} \quad j = i - 1, \quad (12)$$

where $M_n(\cdot)$ in Eq. 10 and in the right-hand side of Eq. 11 indicate the self-test accuracy. $M_n(\cdot)$ in the left-hand side of Eq. 11 indicates the cross-test verification accuracy of the n -th learned model with respect to the previous model (i.e., $j = i - 1$, as shown in Eq. 12). The search is solved online without saving the models learned at previous epochs. In Tab. 5, we compare the basic implementation described in Sec. 7.3, indicated with VANILLA, with the Model Selection

TABLE 5

Dependency of CoReS on Model Selection strategy (MS). CIFAR100 results in sequential ten-model compatibility evaluated in 20 runs. Mean and standard deviation of AC and AM are reported. “Vanilla” represents the default CoReS implementation, in which the no model selection is used. “Model Selection” refers to choose best model solving Eqs. 10-12.

	AC	AM
VANILLA (w/o MS)	0.51 ± 0.10	0.59 ± 0.08
MODEL SELECTION	0.53 ± 0.11	0.59 ± 0.09

strategy indicated with MS. As evidenced by the table, MS increases AC to 0.53 keeping the same AM .

8.3 Model Initialization

At each upgrade we train from scratch by initializing the model with the same random parameters. This implies that all the upgraded models have started their optimization from a common configuration of the weights. In this section, we assess the compatibility when the parameters of the models are randomly initialized at every model upgrade. This implies that all the models are trained starting with a different configuration of the weights. Tab. 6, shows mean and standard deviation of 20 runs of the AC (Eq. 8) and the AM (Eq. 9). As can be noticed, starting from random initialization negatively affects the final performance. In particular, in RANDOM INIT., the AC shows a reduction of 6% and nearly similar AM with respect to the VANILLA training. This positive behavior may be motivated by the observations reported in [61], [62]. They show that initialization, whether pre-trained or random, may have a significant impact on the final classification accuracy and therefore on the learned features. This is most likely related to the concept of “flat minima” and to the fact that with a fixed initialization, the SGD optimization explores the same basin in the loss minimum [63], [64].

8.3.1 Fine-Tuning the Previously Learned Model

We also evaluated CoReS in an *Incremental Fine Tuning* setup in which instead of learning the model from scratch at each upgrade, the weights of the current model are initialized with the ones learned in the previous upgrade. As shown in Fig. 9, there is a substantial reduction in the overall performance with respect to our training procedure shown in Fig. 5(g). This is supposed to be related to the fact that to assimilate novel class knowledge under the compatibility constraint, optimization requires going back

TABLE 6

Ablation of different model initializations. CIFAR100 results of 10-model compatibility evaluated in 20 runs. Mean and standard deviation of AC and AM are reported. “Vanilla” represents the default CoReS implementation, in which at each run the same random initialization is used for each model upgrade. “Random init.” refers to using a different random initialization at each model upgrade.

INITIALIZATION ABLATION	AC	AM
VANILLA (SAME INIT.)	0.51 ± 0.10	0.59 ± 0.08
RANDOM INIT.	0.45 ± 0.09	0.60 ± 0.11

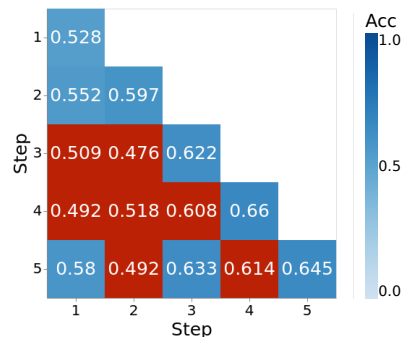


Fig. 9. Sequential five-model compatibility matrix of CoReS with Incremental Fine-tuning (IFT) with models sequentially learned on CIFAR-100. As evidenced from the figure, this does not learn compatible features. The compatibility matrix of CoReS without IFT is shown in Fig. 5(g).

to earlier weight configurations to find more complex error landscapes. This condition can simply be avoided learning the model from scratch.

8.4 Different class orderings

Since compatibility is a sequential learning problem, we evaluate if the order of learning the new upgrades has influence on the learned compatible representation. The ablation is performed in the 10-model compatibility scenario (similar to 7.3) using the CIFAR-100 dataset for learning the compatible representation and CIFAR-10 for evaluating the verification test. We report mean and standard deviation of 20 runs in which at each run a different permutation of the classes is used. We compare it with the VANILLA implementation, where the default alphabetically order of the classes is always used. As shown in Tab. 7 permuting the class order, indicated as RANDOM CLASS ORDER, does not affect the AM and the AC values with respect to the VANILLA implementation of CoReS. The average reduction at the end of the training process is substantially negligible and therefore with no impact on performance. It is however worth noticing that the standard deviation of the AC is one order of magnitude higher of the standard deviation of the AM showing that class orderings more effect on compatibility. This may be caused the high complexity introduced by learning compatible representations.

8.5 Different Model Architectures

In this section, we evaluate the effect of different model architectures on learning compatible representations with

TABLE 7

Ablation of different class order. CIFAR100 results of 10-model compatibility evaluated in 20 runs. Mean and standard deviation of AC and AM are reported. “Vanilla” represents the default CoReS implementation, in which the class alphabetical order is always used. “Random class order” refers to a different random permutation of the classes at each run.

ORDER ABLATION	AC	AM
VANILLA (SAME ORDER)	0.51 ± 0.10	0.59 ± 0.08
RANDOM CLASS ORDER	0.52 ± 0.13	0.57 ± 0.05

CoReS. We study if the stationary constraint imposed by the fixed classifier benefits or limits the use of different architectures. It has been shown that the architecture expressive power improves the classification accuracy of fixed classifiers [44], [46]. According to this, in addition to the SENet-18 architecture evaluated in Sec. 7.3, we ablate the individual contribution of three further architectures: the ResNet with two different depths (20 and 32) and the more recent RegNet [65]⁵. Architectures are selected so as to have increasing expressive power, e.g., recent network design and an increasing number of parameters. Parameters increase as follows: 0.27M, 0.46M, 1.23M and 2.36M for ResNet20, ResNet32, SENet-18 and RegNetX_200MF. In every architecture learning scenario (except the SENet-18), we set the SGD initial learning rate to 0.1 and the weight decay factor is $2 \cdot 10^{-4}$. For the ResNet20 model architecture, we train the model for 40 epochs and we do not decrease the learning rate. For the ResNet32, we train the model for 70 epochs and we decrease the learning rate to 0.01 and to 0.001 at the 50-th and 65-th epoch, respectively. For the RegNetX_200MF, we train the model for 150 epochs and we reduce the learning rate at the 70-th and 120-th epoch to 0.01 and 0.001, respectively. Fig. 10(a), Fig. 10(b) and Fig. 10(c) represent the compatibility matrices of CoReS with the ResNet20, the ResNet32 and the RegNetX_200MF, respectively. For completeness, the SENet-18 is shown in Fig. 5(e). As it can be noticed, both the compatibility and verification accuracy follows the expressive power of the evaluated model architectures. The ResNet32 in Fig. 10(b) has compatibility similar to Fig. 10(a) but the verification is higher. As shown in Fig. 10(c) the RegNetX_200MF architecture both improves the compatibility and the verification metric. This shows that our compatible learning approach is general enough to be applied in a wide range of scale variations and complexity.

8.5.1 Upgrading with Different Model Architectures

We further study the effects of model architecture changes during the model upgrade. This is the practical case in which a deployed system is upgraded not only with fresh data but also with recent and more powerful network architectures. As CoReS learn compatible features by sharing the same representation space of previous and future models irrespective of the layers within the architectures, we ask ourselves whether this might affect the results. According to this, we evaluate the sequential 3-model compatibility upgrading the ResNet20 to the SENet-18, and subsequently to the RegNetX_200MF. Training is performed as in Sec. 8.5. Fig. 10(d) reports the compatibility matrix results of the evaluation. As it can be noticed, the resulting representations are always compatible between ResNet20, SENet-18 and RegNetX_200MF. Also in this case, the increasing expressive power of the architectures is positively reflected on the sequential compatibility performance. Our approach therefore provides a general framework for learning compatible representations that sequentially leverages architectures of increasing expressiveness.

⁵. Code source for ResNet20 and RegNetX_200MF can be found at <https://github.com/kuangliu/pytorch-cifar> and for ResNet32 at https://github.com/arthurdouillard/incremental_learning_pytorch

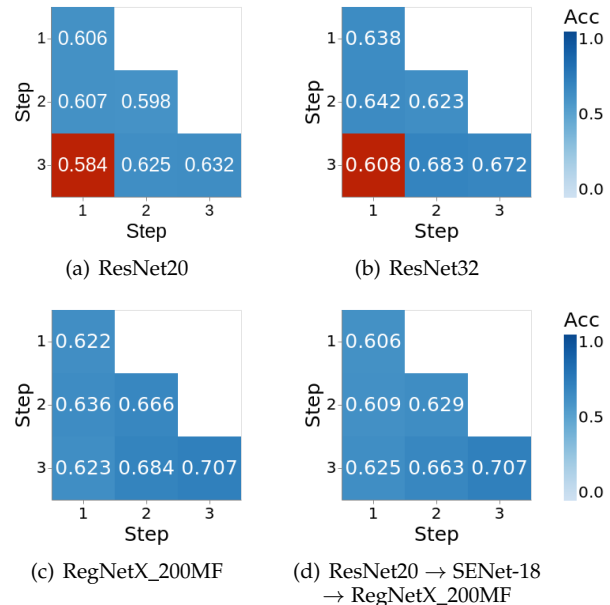


Fig. 10. Evaluation with different model architectures in a 3-model compatibility scenario with CIFAR-100/10. (a), (b), (c) evaluate CoReS with a ResNet20, ResNet32, and RegNetX_200MF architecture, respectively. In (c) is reported the compatibility matrix obtained adopting ResNet20 at the first step, SENet-18 at the second, and finally RegNetX_200MF.

9 CONCLUSIONS

We have presented CoReS, a novel approach to learn compatible representations. Compatible representation allows “new” learned features to be compared directly to “old” features, so they can be used interchangeably in time. This enables Visual Search systems to avoid re-indexing the gallery-set when updating the representation model. CoReS achieved significantly better performance with respect to the current state-of-the-art method in the case of sequential multi-model compatibility. CoReS leverages fixed classifiers based on Regular Polytopes that allows learning stationary representation models without the need for an auxiliary loss imposing pairwise model training.

In a more complex learning setting, the gallery-set can grow to include a new set of images. New training data can also be included in the gallery, depending on whether it has been already seen or not. Eventually, already seen data could be kept or removed from the gallery based on some redundancy criterion [66].

ACKNOWLEDGMENTS

This work was partially supported by the European Commission under European Horizon 2020 Programme, grant number 951911 - AI4Media.

The authors also acknowledge the CINECA award under the ISCRA initiative (ISCRA-C - “ILCoRe”, ID: HP10CRMI87), for the availability of high performance computing resources.

REFERENCES

- [1] Sumit Chopra, Raia Hadsell, and Yann LeCun. Learning a similarity metric discriminatively, with application to face verification.

- In 2005 *IEEE Computer Society Conference on Computer Vision and Pattern Recognition (CVPR'05)*, volume 1, pages 539–546. IEEE, 2005.
- [2] Yoshua Bengio, Aaron Courville, and Pascal Vincent. Representation learning: A review and new perspectives. *IEEE transactions on pattern analysis and machine intelligence*, 35(8):1798–1828, 2013.
 - [3] Ali Sharif Razavian, Hossein Azizpour, Josephine Sullivan, and Stefan Carlsson. Cnn features off-the-shelf: an astounding baseline for recognition. In *Proceedings of the IEEE conference on computer vision and pattern recognition workshops*, pages 806–813, 2014.
 - [4] Jason Yosinski, Jeff Clune, Yoshua Bengio, and Hod Lipson. How transferable are features in deep neural networks? In Z. Ghahramani, M. Welling, C. Cortes, N. Lawrence, and K. Q. Weinberger, editors, *Advances in Neural Information Processing Systems*, volume 27. Curran Associates, Inc., 2014.
 - [5] Florian Schroff, Dmitry Kalenichenko, and James Philbin. Facenet: A unified embedding for face recognition and clustering. In *Proceedings of the IEEE conference on computer vision and pattern recognition*, pages 815–823, 2015.
 - [6] Weiyang Liu, Yandong Wen, Zhiding Yu, and Meng Yang. Large-margin softmax loss for convolutional neural networks. In *Proceedings of the 33rd International Conference on Machine Learning*, pages 507–516, 2016.
 - [7] Yaniv Taigman, Ming Yang, Marc’Aurelio Ranzato, and Lior Wolf. Deepface: Closing the gap to human-level performance in face verification. In *Proceedings of the IEEE conference on computer vision and pattern recognition*, pages 1701–1708, 2014.
 - [8] Yi Sun, Yuheng Chen, Xiaogang Wang, and Xiaoou Tang. Deep learning face representation by joint identification-verification. In Z. Ghahramani, M. Welling, C. Cortes, N. Lawrence, and K. Q. Weinberger, editors, *Advances in Neural Information Processing Systems*, volume 27. Curran Associates, Inc., 2014.
 - [9] Jiankang Deng, Jia Guo, Niannan Xue, and Stefanos Zafeiriou. Arcface: Additive angular margin loss for deep face recognition. In *Proceedings of the IEEE/CVF Conference on Computer Vision and Pattern Recognition*, pages 4690–4699, 2019.
 - [10] Dong Yi, Zhen Lei, Shengcai Liao, and Stan Z Li. Deep metric learning for person re-identification. In *2014 22nd International Conference on Pattern Recognition*, pages 34–39. IEEE, 2014.
 - [11] Wei Li, Rui Zhao, Tong Xiao, and Xiaogang Wang. Deepreid: Deep filter pairing neural network for person re-identification. In *Proceedings of the IEEE conference on computer vision and pattern recognition*, pages 152–159, 2014.
 - [12] Liang Zheng, Hengheng Zhang, Shaoyan Sun, Manmohan Chandraker, Yi Yang, and Qi Tian. Person re-identification in the wild. In *Proceedings of the IEEE Conference on Computer Vision and Pattern Recognition*, pages 1367–1376, 2017.
 - [13] Tianlong Chen, Shaojin Ding, Jingyi Xie, Ye Yuan, Wuyang Chen, Yang Yang, Zhou Ren, and Zhangyang Wang. Abd-net: Attentive but diverse person re-identification. In *Proceedings of the IEEE/CVF International Conference on Computer Vision*, pages 8351–8361, 2019.
 - [14] Artem Babenko, Anton Slesarev, Alexandr Chigorin, and Victor Lempitsky. Neural codes for image retrieval. In *European conference on computer vision*, pages 584–599. Springer, 2014.
 - [15] Albert Gordo, Jon Almazán, Jerome Revaud, and Diane Larlus. Deep image retrieval: Learning global representations for image search. In *European conference on computer vision*, pages 241–257. Springer, 2016.
 - [16] Giorgos Tolias, Ronan Sifre, and Hervé Jégou. Particular Object Retrieval With Integral Max-Pooling of CNN Activations. In *ICLR 2016 - International Conference on Learning Representations*, International Conference on Learning Representations, pages 1–12, San Juan, Puerto Rico, May 2016.
 - [17] Giorgos Tolias, Ronan Sifre, and Hervé Jégou. Particular Object Retrieval With Integral Max-Pooling of CNN Activations. In *ICLR 2016 - International Conference on Learning Representations*, International Conference on Learning Representations, pages 1–12, San Juan, Puerto Rico, May 2016.
 - [18] Dharshan Kumaran, Demis Hassabis, and James L McClelland. What learning systems do intelligent agents need? complementary learning systems theory updated. *Trends in cognitive sciences*, 20(7):512–534, 2016.
 - [19] Aida Nematzadeh, Sebastian Ruder, and Dani Yogatama. On memory in human and artificial language processing systems. In *Proceedings of the Bridging AI and Cognitive Science Workshop at ICLR*, 2020.
 - [20] Edmund T Rolls. Memory systems in the brain. *Annual review of psychology*, 51(1):599–630, 2000.
 - [21] Richard Van Noorden. The ethical questions that haunt facial-recognition research. *Nature*, 587(7834):354–358, 2020.
 - [22] Yantao Shen, Yuanjun Xiong, Wei Xia, and Stefano Soatto. Towards backward-compatible representation learning. In *Proceedings of the IEEE/CVF Conference on Computer Vision and Pattern Recognition*, pages 6368–6377, 2020.
 - [23] Rahul Duggal, Hao Zhou, Shuo Yang, Yuanjun Xiong, Wei Xia, Zhuowen Tu, and Stefano Soatto. Compatibility-aware heterogeneous visual search. In *Proceedings of the IEEE/CVF Conference on Computer Vision and Pattern Recognition*, pages 10723–10732, 2021.
 - [24] Ken Chen, Yichao Wu, Haoyu Qin, Ding Liang, Xuebo Liu, and Junjie Yan. R3 adversarial network for cross model face recognition. In *Proceedings of the IEEE/CVF Conference on Computer Vision and Pattern Recognition*, pages 9868–9876, 2019.
 - [25] Jie Hu, Rongrong Ji, Hong Liu, Shengchuan Zhang, Cheng Deng, and Qi Tian. Towards visual feature translation. In *Proceedings of the IEEE/CVF Conference on Computer Vision and Pattern Recognition*, pages 3004–3013, 2019.
 - [26] Chien-Yi Wang, Ya-Liang Chang, Shang-Ta Yang, Dong Chen, and Shang-Hong Lai. Unified representation learning for cross model compatibility. In *31st British Machine Vision Conference 2020, BMVC 2020, Virtual Event, UK, September 7-10, 2020*. BMVA Press, 2020.
 - [27] Qiang Meng, Chixiang Zhang, Xiaoqiang Xu, and Feng Zhou. Learning compatible embeddings. In *Proceedings of the IEEE/CVF International Conference on Computer Vision (ICCV)*, pages 9939–9948, October 2021.
 - [28] Federico Pernici, Matteo Bruni, Claudio Baccchi, Francesco Turchini, and Alberto Del Bimbo. Class-incremental learning with pre-allocated fixed classifiers. In *25th International Conference on Pattern Recognition, ICPR 2020, Milan, Italy, January 10-15, 2021*. IEEE Computer Society, 2020.
 - [29] Yen-Chang Hsu, Yen-Cheng Liu, Anita Ramasamy, and Zsolt Kira. Re-evaluating continual learning scenarios: A categorization and case for strong baselines. In *NeurIPS Continual Learning Workshop*, 2018.
 - [30] Guido M Van de Ven and Andreas S Tolias. Three scenarios for continual learning. *arXiv preprint arXiv:1904.07734*, 2019.
 - [31] Gagan Bansal, Besmira Nushi, Ece Kamar, Daniel S Weld, Walter S Lasecki, and Eric Horvitz. Updates in human-ai teams: Understanding and addressing the performance/compatibility tradeoff. In *Proceedings of the AAAI Conference on Artificial Intelligence*, volume 33, pages 2429–2437, 2019.
 - [32] Megha Srivastava, Besmira Nushi, Ece Kamar, Shital Shah, and Eric Horvitz. An empirical analysis of backward compatibility in machine learning systems. In *Proceedings of the 26th ACM SIGKDD International Conference on Knowledge Discovery & Data Mining*, pages 3272–3280, 2020.
 - [33] Sijie Yan, Yuanjun Xiong, Kaustav Kundu, Shuo Yang, Siqi Deng, Meng Wang, Wei Xia, and Stefano Soatto. Positive-congruent training: Towards regression-free model updates. In *Proceedings of the IEEE/CVF Conference on Computer Vision and Pattern Recognition*, pages 14299–14308, 2021.
 - [34] F. Träuble, J. von Kügelgen, M. Kleindessner, F. Locatello, B. Schölkopf, and P. Gehler. Backward-compatible prediction updates: A probabilistic approach. In *Advances in Neural Information Processing Systems 34 (NeurIPS 2021)*, December 2021.
 - [35] Michael Gygli, Jasper Uijlings, and Vittorio Ferrari. Towards reusable network components by learning compatible representations. In *Proceedings of the AAAI Conference on Artificial Intelligence*, volume 35, pages 7620–7629, 2021.
 - [36] Yixuan Li, Jason Yosinski, Jeff Clune, Hod Lipson, and John Hopcroft. Convergent learning: Do different neural networks learn the same representations? In *Feature Extraction: Modern Questions and Challenges*, pages 196–212. PMLR, 2015.
 - [37] Liwei Wang, Lunjia Hu, Jiayuan Gu, Yue Wu, Zhiqiang Hu, Kun He, and John Hopcroft. Towards understanding learning representations: To what extent do different neural networks learn the same representation. In *Proceedings of the 32nd International Conference on Neural Information Processing Systems, NIPS’18*, page 9607–9616, Red Hook, NY, USA, 2018. Curran Associates Inc.
 - [38] Marc Masana, Xialei Liu, Bartłomiej Twardowski, Mikel Menta, Andrew D Bagdanov, and Joost van de Weijer. Class-incremental learning: survey and performance evaluation. *arXiv preprint arXiv:2010.15277*, 2020.

- [39] Michael McCloskey and Neal J Cohen. Catastrophic interference in connectionist networks: The sequential learning problem. In *Psychology of learning and motivation*, volume 24, pages 109–165. Elsevier, 1989.
- [40] Yandong Wen, Kaipeng Zhang, Zhifeng Li, and Yu Qiao. A discriminative feature learning approach for deep face recognition. In *European Conference on Computer Vision*, pages 499–515. Springer, 2016.
- [41] Yann LeCun, Léon Bottou, Yoshua Bengio, and Patrick Haffner. Gradient-based learning applied to document recognition. *Proceedings of the IEEE*, 86(11):2278–2324, 1998.
- [42] Weiyang Liu, Yandong Wen, Zhiding Yu, and Meng Yang. Large-margin softmax loss for convolutional neural networks. In Maria-Florina Balcan and Kilian Q. Weinberger, editors, *Proceedings of the 33rd International Conference on Machine Learning, ICML 2016, New York City, NY, USA, June 19–24, 2016*, volume 48 of *JMLR Workshop and Conference Proceedings*, pages 507–516. JMLR.org, 2016.
- [43] Weiyang Liu, Yandong Wen, Zhiding Yu, Ming Li, Bhiksha Raj, and Le Song. SpheroFace: Deep hypersphere embedding for face recognition. In *2017 IEEE Conference on Computer Vision and Pattern Recognition, CVPR 2017, Honolulu, HI, USA, July 21–26, 2017*, pages 6738–6746. IEEE Computer Society, 2017.
- [44] F. Pernici, M. Bruni, C. Baccchi, and A. D. Bimbo. Regular polytope networks. *IEEE Transactions on Neural Networks and Learning Systems*, pages 1–15, 2021.
- [45] Harold Scott Macdonald Coxeter. *Regular polytopes*. Courier Corporation, 1973.
- [46] Elad Hoffer, Itay Hubara, and Daniel Soudry. Fix your classifier: the marginal value of training the last weight layer. *arXiv preprint arXiv:1801.04540*, 2018.
- [47] David Lopez-Paz and Marc’Aurelio Ranzato. Gradient episodic memory for continual learning. *Advances in neural information processing systems*, 30:6467–6476, 2017.
- [48] Zhizhong Li and Derek Hoiem. Learning without forgetting. *IEEE transactions on pattern analysis and machine intelligence*, 40(12):2935–2947, 2017.
- [49] Walter J Scheirer, Anderson de Rezende Rocha, Archana Sapkota, and Terrance E Boulton. Toward open set recognition. *IEEE transactions on pattern analysis and machine intelligence*, 35(7):1757–1772, 2012.
- [50] Alex Krizhevsky, Geoffrey Hinton, et al. Learning multiple layers of features from tiny images. *Citeseer*, 2009.
- [51] Dong Yi, Zhen Lei, Shengcai Liao, and Stan Z Li. Learning face representation from scratch. *arXiv preprint arXiv:1411.7923*, 2014.
- [52] Gary B. Huang, Manu Ramesh, Tamara Berg, and Erik Learned-Miller. Labeled faces in the wild: A database for studying face recognition in unconstrained environments. Technical Report 07-49, University of Massachusetts, Amherst, October 2007.
- [53] Liang Zheng, Liyue Shen, Lu Tian, Shengjin Wang, Jingdong Wang, and Qi Tian. Scalable person re-identification: A benchmark. In *Proceedings of the IEEE international conference on computer vision*, pages 1116–1124, 2015.
- [54] Jie Hu, Li Shen, Samuel Albanie, Gang Sun, and Enhua Wu. Squeeze-and-excitation networks. *IEEE Transactions on Pattern Analysis and Machine Intelligence*, 42(8):2011–2023, 2020.
- [55] Kaiming He, Xiangyu Zhang, Shaoqing Ren, and Jian Sun. Deep residual learning for image recognition. In *Proceedings of the IEEE conference on computer vision and pattern recognition*, pages 770–778, 2016.
- [56] Kaiyang Zhou and Tao Xiang. Torchreid: A library for deep learning person re-identification in pytorch. *arXiv preprint arXiv:1910.10093*, 2019.
- [57] Diederik P Kingma and Jimmy Ba. Adam: A method for stochastic optimization. *arXiv preprint arXiv:1412.6980*, 2014.
- [58] Joaquin Quiñero-Candela, Masashi Sugiyama, Neil D Lawrence, and Anton Schwaighofer. *Dataset shift in machine learning*. MIT Press, 2009.
- [59] Masashi Sugiyama, Matthias Krauledat, and Klaus-Robert Müller. Covariate shift adaptation by importance weighted cross validation. *Journal of Machine Learning Research*, 8(5), 2007.
- [60] Mervyn Stone. Cross-validatory choice and assessment of statistical predictions. *Journal of the royal statistical society: Series B (Methodological)*, 36(2):111–133, 1974.
- [61] Vaishnavh Nagarajan and J. Zico Kolter. Uniform convergence may be unable to explain generalization in deep learning. In H. Wallach, H. Larochelle, A. Beygelzimer, F. d’Alché-Buc, E. Fox,

and R. Garnett, editors, *Advances in Neural Information Processing Systems*, volume 32. Curran Associates, Inc., 2019.

- [62] Behnam Neyshabur, Hanie Sedghi, and Chiyuan Zhang. What is being transferred in transfer learning? In *NeurIPS*, 2020.
- [63] Sepp Hochreiter and Jürgen Schmidhuber. Simplifying neural nets by discovering flat minima. In *Advances in neural information processing systems*, pages 529–536, 1995.
- [64] Sepp Hochreiter and Jürgen Schmidhuber. Flat minima. *Neural computation*, 9(1):1–42, 1997.
- [65] Ilija Radosavovic, Raj Prateek Kosaraju, Ross Girshick, Kaiming He, and Piotr Dollár. Designing network design spaces. In *Proceedings of the IEEE/CVF Conference on Computer Vision and Pattern Recognition*, pages 10428–10436, 2020.
- [66] Federico Pernici, Federico Bartoli, Matteo Bruni, and Alberto Del Bimbo. Memory based online learning of deep representations from video streams. In *Proceedings of the IEEE Conference on Computer Vision and Pattern Recognition*, pages 2324–2334, 2018.



Niccolò Biondi Niccolò Biondi received the M.S. degree (cum laude) in Computer Engineering from the University of Firenze, Italy, in 2021. Presently, he is a Ph.D. student at the University of Firenze at MICC, Media Integration and Communication Center, University of Firenze. His research interests include machine learning and computer vision with special focus on compatible learning, representation learning, and incremental learning.



Federico Pernici Federico Pernici received the laurea degree in Information Engineering in 2002, the post-laurea degree in Internet Engineering in 2003 and the Ph.D. in Information and Telecommunication Engineering in 2005 from the University of Firenze, Italy. Since 2002 he has been a research assistant at MICC Media Integration and Communication Center, assistant professor and adjunct professor at the University of Firenze. His scientific interests are computer vision and machine learning with a focus on

different aspects of visual tracking, incremental learning and representation learning. Presently, he is Associate Editor of *Machine Vision and Applications* journal.



Matteo Bruni Matteo Bruni received the M.S. degree (cum laude) in Computer Engineering from the University of Firenze, Italy, in 2016, the Ph.D. in Information Engineering at the University of Firenze in 2020. His research interests include pattern recognition and computer vision with specific focus on feature embedding, face recognition, incremental learning and compatible representation.



Alberto Del Bimbo Prof. Del Bimbo is Full Professor at the University of Firenze, Italy and the Director of MICC Media Integration and Communication Center. He is the author of over 350 scientific publications in computer vision and multimedia and principal investigator of technology transfer projects with industry and governments. He was the Program Chair of ICPR 2012, ICPR 2016 and ACM Multimedia 2008, and the General Chair of IEEE ICMCS 1999, ACM Multimedia 2010, ICMR 2011 and ECCV 2012. He is the General Chair of the forthcoming ICPR 2020. He is the Editor in Chief of *ACM TOMM Transactions on Multimedia Computing Communications and Applications* and Associate Editor of *Multimedia Tools and Applications* and *Pattern Analysis and Applications* journals. He was Associate Editor of *IEEE Transactions on Pattern Analysis and Machine Intelligence*, *IEEE Transactions on Multimedia* and *Pattern Recognition* and also served as the Guest Editor of many Special Issues in highly ranked journals. Prof. Del Bimbo is IAPR Fellow and ACM Distinguished Scientist and is the recipient of the 2016 ACM SIGMM Award for *Outstanding Technical Contributions to Multimedia Computing Communications and Applications*.